



INFLUENCE OF COMPOSITE MATERIALS ON THE ELECTRIC FIELD DISTRIBUTION OF A HIGH VOLTAGE CABLE

Faouzi HASSAINE ^{1,*} , Lakhdar MADANI ² , Nacereddine GUETTAF ¹ , Samira BOUMOUS ³ ,
Hamou NOURI ¹ 

¹ Department of Electrical Engineering, LAS Laboratory, Ferhat Abbas Setif 1 University, Setif, Algeria

² Department of Electrical Engineering, DAC HR Laboratory, Ferhat Abbas Setif 1 University, Setif, Algeria

³ Department of Electrical Engineering, LEERE Laboratory, Mohamed Cherif Messaïdia University, Souk Ahras, Algeria

*Correspondance e-mail: faouzi.hassaine@univ-setif.dz

Abstract

Our significant contribution is to bring improvements to the level of existing formulations for the different layers of high-voltage underground cables using the concept of composite. This paper is focused on studying the impact of additives on the electric field behaviour in the different dielectric layers of a three-core XLPE power cable using Matlab software and a finite element approach in COMSOL Multiphysics software. This study is an extension of previous studies only interested in the insulating part of the cables. The reduction in the electric field with the augmentation of fillers was observed, and it's very significant in insulating layers. In semiconducting layers, it also leads to an increase in the electric field in the insulation layers. While in the other dielectrics layers, there is no effect. The results indicate that the electric field strength could be controlled by adjusting the relative permittivity of the dielectrics by adding single or multiple particles.

Keywords: power cable, dielectric composite materials, electric field, permittivity, COMSOL Multiphysics software

List of Symbols/Acronyms

C – Natural Graphite;
EPR – Ethylene Propylene Rubber;
FEM – Finite Element Method;
Ge – Germanium;
HV – High Voltage;
PVC – Polyvinyl Chloride;
q – Material's Volume Fraction;
 $q_{(i,n)}$ – Material's Volume Fraction of the i^{th} Composite Component;
Si – Silicon;
XLPE – Cross-linked Polyethylene;
ZnO – Zinc Oxide;
 ε_{eff} – Effective Relative Permittivity of the Composite Materials;
 $\varepsilon_{(i,n)}$ – Material's Relative Permittivity of i^{th} Composite Component;
 ε_r – Relative Permittivity of the Medium;
 ε_0 – Permittivity of Free Space;
 ε_1 – Matrix's Relative Permittivity of the Composite Materials;
 ε_2 – Inclusion's Relative Permittivity of the Composite Materials;
E – Electric Field [V/m];
D – Electrical Displacement [C/m²];
F – Frequency [Hz];
 ρ – Free Charge Density [C/m³].

1. INTRODUCTION

In recent years, there has been significant growth in the usage of underground power cables in both distribution and transmission networks. The use of electrical cables is growing rapidly due to the growing requirement for electrical energy and the expanding resident density in various areas. Compared to overhead transmission lines, power cables are more often employed in downtown distribution networks due to the simplicity of installation and absence of interference with the appearance of the city throughout installation [1], their visual effect, intense civil opposition, the difficulties of expropriating the damaged land within in the project's timeline and cost constraints etc [1, 2].

Three-core underground power cables have certain advantages over the utilisation of three underground power cables in technical and economic terms, such as minimisation of losses, reduction in the cost of cable manufacture, weight, and space occupied by the cable to transmit the same power. Polymers are mostly employed as functional materials [3] and have been extensively employed as electrical insulation materials for underground

cables since the early 20th century because of their dependability, availability, simplicity of manufacturing, low costs [4, 5], their lightweight nature, impact resistance and show a good vibration damping performance [3]. Among polymeric materials, cross-linked polyethylene (XLPE) possesses the finest insulating properties [6]. Indeed, high-voltage power cables usually use cross-linked polyethylene (XLPE) as insulation material [6,7] and are also employed in extra-high-voltage cables in addition to low and medium-voltage cables [6]. The high electric field, elevated temperatures, and mechanical stress lead the insulation materials to deteriorate and eventually cause dielectric breakdown over a long period [8].

To enhance the performance of electrical cables, additive materials can be integrated into the polymeric insulating material to generate so-called polymer composites [9]. Today, a wide range of industries sectors use composite materials, and the study of their behaviour is becoming more and more crucial. In comparison to traditional materials, they have more advantages, such as high specific strength and stiffness, high fatigue performance and corrosion resistance [10].

Composite materials typically consist of two or more components having considerably different physical and/or chemical characteristics. The controlled combination of the components results in new materials with different properties from those of the individual components [11, 12]. In addition, composite materials are now often defined as an arrangement of reinforcements (also called fillers) embedded in a matrix [12]. Recently, considerable research has focused on developing these materials using the composite concept to improve their properties and increase the life and reliability of these insulators in high-voltage underground cables [9, 13-17]. But these studies are only interested in the insulating part of high-voltage underground cables. This paper is based on the study of the impact of additive materials such as natural graphite (C) and zinc oxide (ZnO) on the electric field behaviour in the different dielectric layers, as well as germanium (Ge) and natural graphite (C) in the different semiconducting layers of a 33 kV high-voltage three core electric cable. The electrical cable model is created in COMSOL Multiphysics software using the finite element approach.

Due to its very low dielectric loss factor, which keeps constant throughout its entire operating lifetime, and the excellent properties of the XLPE insulation material, it is firmly longitudinally spliced with an inner and outer screen of semi-conductive material; the cable has high operational reliability. It is used in transformer stations, switchgear, power plants, and industrial installations [18].

2. MODEL GEOMETRY AND SIMULATION PARAMETERS

Figure 1 illustrates a three-core high-voltage underground cable with XLPE insulation and steel wire armouring CU / XLPE/ SWA/ PVC 33 kV, $3 \times 70 \text{ mm}^2$ [18].



Fig. 1. Three-core high-voltage power cable with XLPE insulation and steel wire armouring [18]

Figure 2 illustrates the geometry of a 2D model that corresponds to the simulation case study. It shows the cross-section of a three-core high-voltage power underground cable.

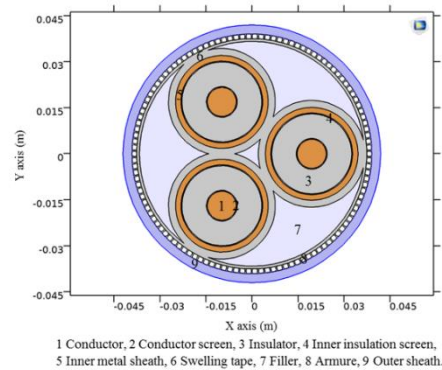


Fig. 2. The geometry of the 2D model of the HV cable cross-section

Tables (1, 2) summarise the geometric quantities and physical parameters of the cable materials necessary to define the medium and the subdomain, respectively.

Table 1. Technical specification of high-voltage underground cable 33 kV [18]

Parameters	Values [mm]
Diameter of conductor	9.43
The thickness of the conductor screen	0.3
The thickness of insulation (XLPE)	8
The thickness of the insulation screen	0.3
Inner sheath thickness	1.8
Armour wire diameter	3.15
The thickness of the outer PVC sheath	3.6
The approximate cable overall diameter	84

Table 2. The electrical characteristics of materials used for a 33 kV XLPE underground Cable [18-25]

Components	Materials	Electrical relative Permittivity	Electrical Conductivity [S/m]	Electrical Resistivity [Ohm.m]
Conductor	Copper	1	5.96×10^7	1.677×10^{-8}
Semiconducting layers	Silicon	11.9	4.347×10^{-4}	2.3×10^3
Insulation	XLPE	2.3	10^{-18}	10^{18}
Inner metallic sheath	Copper	1	5.96×10^7	1.677×10^{-8}
Filler, Swelling tape	EPR	2.35	10^{-15}	10^{15}
Armour copper wire	Galvanized steel wire	1	6.2×10^6	1.61×10^{-7}
Outer sheath	PVC	3	10^{-15}	10^{15}

3. MATHEMATICAL MODELING

In COMSOL Multiphysics, a two-dimensional model is created. It employs the finite element method (FEM), which converts the intended model into a mesh of several elements. It's employed to calculate the values of each point in the model to get precise results. There are several software modules. The AC/DC module and electrostatic subdivision were employed in this analysis to determine the cable's potential and electric field distributions [26].

The electric field E could be obtained from the negative gradient scalar potential V , as written in (1) below [26]:

$$E = -\nabla V \quad (1)$$

The following formula (2) relates the electric displacement D to the electric field E :

$$D = \varepsilon_0 \varepsilon_r E \quad (2)$$

Where ε_r denotes the insulating medium's relative permittivity.

The relationship between electrical displacement D and a free charge density ρ may be computed using Gauss's law as follows:

$$\nabla \cdot D = \rho \quad (3)$$

Hence, the Poisson equation can be expressed in terms of scalar electric potential calculated as indicate in equation 4:

$$\nabla^2 V = -\frac{\rho}{\varepsilon} \quad (4)$$

Assuming that the issue is two-dimensional, (4) may alternatively be written as follows [25]:

$$\frac{\partial^2 V}{\partial x^2} + \frac{\partial^2 V}{\partial y^2} = -\frac{\rho}{\varepsilon} \quad (5)$$

The core voltages are a balanced three-core set at a frequency $f = 50$ Hz and are given below:

$$V_1 = V_0 \quad (6)$$

$$V_2 = V_0 \cdot e^{-\frac{j2\pi}{3}} \quad (7)$$

$$V_3 = V_0 \cdot e^{+\frac{j2\pi}{3}} \quad (8)$$

In this study, the RMS value of the line voltage is 33 kV, so:

$$V_0 = \frac{33}{\sqrt{3}} \text{ kV} \quad (9)$$

The effective permittivity of a binary dielectric mixture is determined using Bruggeman's model. The presumption that explicit host content exists no more exists. Rather, the particles of every single material component are expected to be enclosed in an effective medium whose permittivity equals the permittivity of the mixture ε_{eff} that we are attempting to determine [27]. Thus, must be determined from the relationship [28]:

$$(1 - q) \frac{\varepsilon_1 - \varepsilon_{\text{eff}}}{\varepsilon_1 + 2\varepsilon_{\text{eff}}} + q \frac{\varepsilon_2 - \varepsilon_{\text{eff}}}{\varepsilon_2 + 2\varepsilon_{\text{eff}}} = 0 \quad (10)$$

A general form of the Böttcher equation for a multi-phase system is given by [29]:

$$\sum_{i=1}^n q_i \frac{\varepsilon_i - \varepsilon_{\text{eff}}}{\varepsilon_i + 2\varepsilon_{\text{eff}}} = 0 \quad (11)$$

4. RESULTS AND DISCUSSION

Composite materials can be used to improve the performance of electrical cables and offer many advantages, such as the minimisation of microscopic defects, low dielectric loss, and long service life. Tables (3, 4) below show the calculated dielectric permittivities of the different layers of the cable according to the concentration of the individual and multiple additive materials.

To acquire accurate findings through finite element analysis, the critical regions are subdivided into tiny regions named elements, referred to as meshing, as seen in Figure 3.

3. MATHEMATICAL MODELING

In COMSOL Multiphysics, a two-dimensional model is created. It employs the finite element method (FEM), which converts the intended model into a mesh of several elements. It's employed to calculate the values of each point in the model to get precise results. There are several software modules. The AC/DC module and electrostatic subdivision were employed in this analysis to determine the cable's potential and electric field distributions [26].

The electric field E could be obtained from the negative gradient scalar potential V , as written in (1) below [26]:

$$E = -\nabla V \quad (1)$$

The following formula (2) relates the electric displacement D to the electric field E :

$$D = \varepsilon_0 \varepsilon_r E \quad (2)$$

Where ε_r denotes the insulating medium's relative permittivity.

The relationship between electrical displacement D and a free charge density ρ may be computed using Gauss's law as follows:

$$\nabla \cdot D = \rho \quad (3)$$

Hence, the Poisson equation can be expressed in terms of scalar electric potential calculated as indicate in equation 4:

$$\nabla^2 V = -\frac{\rho}{\varepsilon} \quad (4)$$

Assuming that the issue is two-dimensional, (4) may alternatively be written as follows [25]:

$$\frac{\partial^2 V}{\partial x^2} + \frac{\partial^2 V}{\partial y^2} = -\frac{\rho}{\varepsilon} \quad (5)$$

The core voltages are a balanced three-core set at a frequency $f = 50$ Hz and are given below:

$$V_1 = V_0 \quad (6)$$

$$V_2 = V_0 \cdot e^{-\frac{j2\pi}{3}} \quad (7)$$

$$V_3 = V_0 \cdot e^{+\frac{j2\pi}{3}} \quad (8)$$

In this study, the RMS value of the line voltage is 33 kV, so:

$$V_0 = \frac{33}{\sqrt{3}} \text{ kV} \quad (9)$$

The effective permittivity of a binary dielectric mixture is determined using Bruggeman's model. The presumption that explicit host content exists no more exists. Rather, the particles of every single material component are expected to be enclosed in an effective medium whose permittivity equals the permittivity of the mixture ε_{eff} that we are attempting to determine [27]. Thus, must be determined from the relationship [28]:

$$(1 - q) \frac{\varepsilon_1 - \varepsilon_{\text{eff}}}{\varepsilon_1 + 2\varepsilon_{\text{eff}}} + q \frac{\varepsilon_2 - \varepsilon_{\text{eff}}}{\varepsilon_2 + 2\varepsilon_{\text{eff}}} = 0 \quad (10)$$

A general form of the Böttcher equation for a multi-phase system is given by [29]:

$$\sum_{i=1}^n q_i \frac{\varepsilon_i - \varepsilon_{\text{eff}}}{\varepsilon_i + 2\varepsilon_{\text{eff}}} = 0 \quad (11)$$

4. RESULTS AND DISCUSSION

Composite materials can be used to improve the performance of electrical cables and offer many advantages, such as the minimisation of microscopic defects, low dielectric loss, and long service life. Tables (3, 4) below show the calculated dielectric permittivities of the different layers of the cable according to the concentration of the individual and multiple additive materials.

To acquire accurate findings through finite element analysis, the critical regions are subdivided into tiny regions named elements, referred to as meshing, as seen in Figure 3.

Table 3. The dielectric permittivities of the different cable layers depend on the concentration of the individual additive materials

Materials Concentrations Additive materials	Semiconductor Si		Insulation XLPE		Common screen EPR		Outer sheath PVC	
	C	Ge	C	ZnO	C	ZnO	C	ZnO
0 %	11.9		2.3		2.35		3	
2.5 %	11.971	11.992	2.4160	2.3853	2.4674	2.4358	3.1326	3.0892
5 %	12.043	12.085	2.5410	2.4748	2.5937	2.5256	3.2735	3.1816
7.5 %	12.115	12.178	2.6757	2.5684	2.7297	2.6196	3.4231	3.2770
10 %	12.188	12.272	2.8206	2.6664	2.8759	2.7178	3.5818	3.3756
12.5 %	12.261	12.367	2.9765	2.7687	3.0329	2.8203	3.7500	3.4774
15 %	12.334	12.462	3.1441	2.8756	3.2015	2.9272	3.9280	3.5824
17.5 %	12.407	12.557	3.3237	2.9869	3.3820	3.0385	4.1146	3.6907
20 %	12.481	12.654	3.5161	3.1029	3.5750	3.1543	4.3147	3.8021
22.5 %	12.555	12.750	3.7215	3.2235	3.7809	3.2746	4.5237	3.9167
25 %	12.629	12.847	3.9403	3.3487	4	3.3994	4.7434	4.0345
27.5 %	12.704	12.945	4.1727	3.4784	4.2324	3.5286	4.9737	4.1554
30 %	12.779	13.044	4.4188	3.6127	4.4782	3.6631	5.2147	4.2795

Where:

Ge: Germanium has a dielectric permittivity of 16 [20];

C: Natural graphite has an equal dielectric permittivity of 12-15 [30];

ZnO: Zinc oxide has a dielectric permittivity of 8.75 [31].

Table 4. The dielectric permittivities of the several layers of the cable as a function of the concentration of the multiple additive materials

Materials Concentrations of additive materials	Semiconductor Si	Insulation XLPE	Common screen EPR	Outer sheath PVC
0 %	11.9	2.3	2.35	3
2.5 % Ge, 2.5 % C	12.064	2.507	2.559	3.227
5 % Ge, 5 % C	12.230	2.741	2.795	3.476
7.5 % Ge, 7.5 % C	12.398	3.004	3.058	3.748
10 % Ge, 10 % C	12.567	3.298	3.353	4.045
12.5 % Ge, 12.5 % C	12.738	3.623	3.679	4.366
15 % Ge, 15 % C	12.911	3.983	4.037	4.713

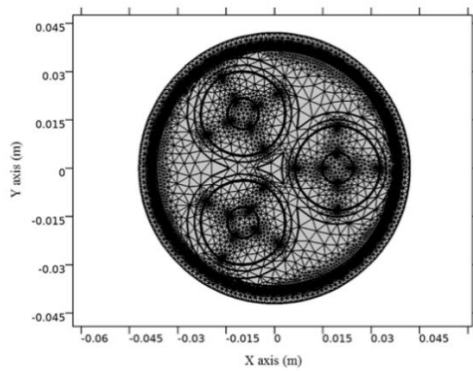


Fig. 3. The meshing geometric model of a three-core high-voltage underground cable with XLPE insulation and steel wire armouring

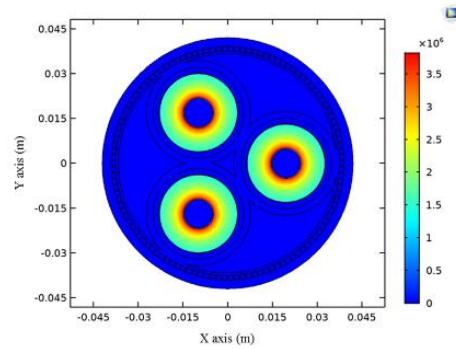


Fig. 5. Electric field distribution in three-core XLPE high-voltage underground cable model

4.1. Electric potential distribution

The simulation model of the electric potential distribution is shown in Figure 4.

Figure 4 shows the electrical distribution potential for the underground cable model. Considering the variations in the phase angle of the

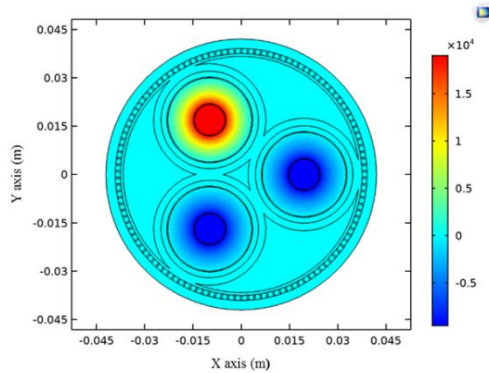


Fig. 4. Electric potential distribution in three-core XLPE high-voltage underground cable model

applied electric potential at each core, this situation is expected. The electric potential distribution is higher and constant inside the core and decreases as a function of the radius around the different cable layers. It is weak at the end of the cable.

4.2. Electric field distribution

The simulation model of the electric field distribution is illustrated in Figure 5.

We can observe the rotational symmetry of the electric field around the three conductors, which is expected due to the symmetry of the cable. The electric field inside the core is null, whereas the electric field strength distribution near the core is high, reaches its maximum value, and becomes lower at the cable's ending. It decreased as a function of cable radius.

The following results illustrate the impact of individual and multiple additive materials in the different dielectric layers of the high-voltage underground cable on the behaviour of the electric field distribution with several concentrations.

4.2.1. The effect of additive materials in the inner semiconducting layer

In order to study the impact of additive materials in the inner semiconducting layer on the electric field behaviour in the cable. Figures (6, 7, 8) illustrate the electric field behaviour inside high-voltage underground cables by adding additive materials with several concentrations, which the variant is the internal semi-conductive layer of pure silicon (Si) and composites with germanium (Ge), natural graphite (C), and multiple, respectively.

Figures (9, 10) show the maximum electric field strength in the inner semiconducting layer and the insulating layer, respectively, as a function of additive material concentration.

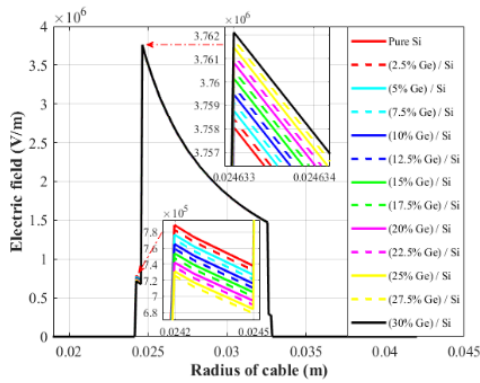


Fig. 6. Effect of germanium in the inner semiconducting layer on the electric field behaviour in the cable

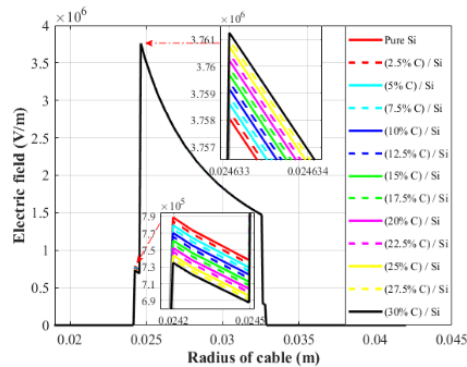


Fig. 7. Effect of natural graphite in the inner semiconducting layer on the electric field behaviour in the cable

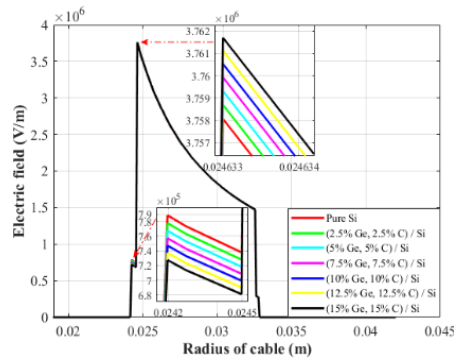


Fig. 8. Effect of germanium and natural graphite in the inner semiconducting layer on the electric field behaviour in the cable

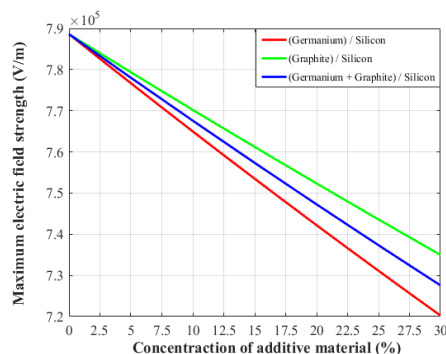


Fig. 9. The maximum electric field strength in the inner semiconducting layer as a function of additive materials concentration

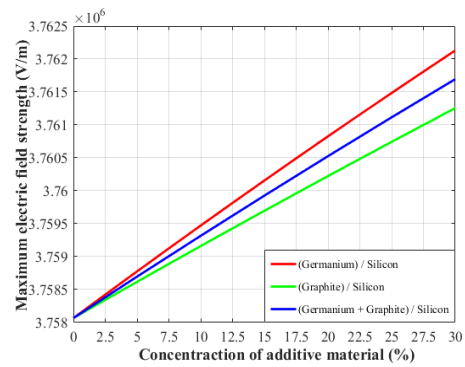


Fig. 10. The maximum electric field strength in the insulating layer as a function of additive materials concentration

In the area corresponding to the internal semiconducting ($x: 0.0242 - 0.0245$ m, $y: 0 - 0.042$ m), it can be seen that the electric field distribution decreases with increasing concentration of the individual and multiple additive materials; as the electric field strength in the case of pure silicon reaches 788.616 kV/m in this area, it decreases as a function of germanium, natural graphite, and multiple, it reaches 720.249 kV/m approximately 8.67 %, 734.986 kV/m around 6.80 %, and 727.573 kV/m about 7.74 %, respectively, at 30 % of the concentration of additive materials.

However, in the area corresponding to the insulating part of the high-voltage cable ($x: 0.0245 - 0.0325$ m, $y: 0 - 0.042$ m), where the electric field distribution is maximum, it can be seen that the electric field distribution increases with increasing concentration of the individual and multiple additive materials as the electric field strength in the case of pure silicon reaches 3758.066 kV/m in this area, it increases as a function of germanium, natural graphite, and multiple, it reaches 3762.130 kV/m approximately 0.108 %, 3761.254 kV/m around 0.084 %, and 3761.695 kV/m close to 0.096 %, respectively, at 30 % of the concentration of additive materials.

4.2.2. The effect of additive materials in the insulating layer

In order to study the impact of additive materials in the insulating layer on the electric field behaviour in the cable. Figures (11, 12, 13) illustrate the electric field behaviour inside high-voltage underground cables by adding additive materials with several concentrations, which the variant is pure cross-linked polyethylene (XLPE) insulating layer and natural graphite (C), zinc oxide (ZnO), and multiple composites, respectively.

Figure 14 shows the maximum electric field strength in the insulating layer as a function of additive material concentration.

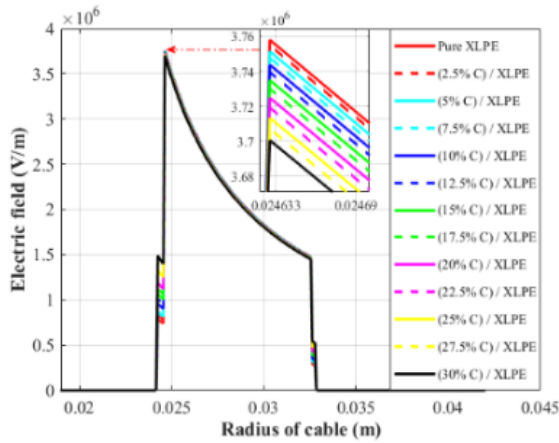


Fig. 11. Effect of natural graphite in the insulating layer on the electric field behaviour in the cable

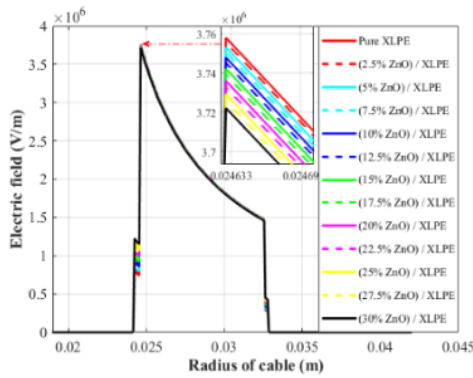


Fig. 12. Effect of zinc oxide in the insulating layer on the electric field behaviour in the cable

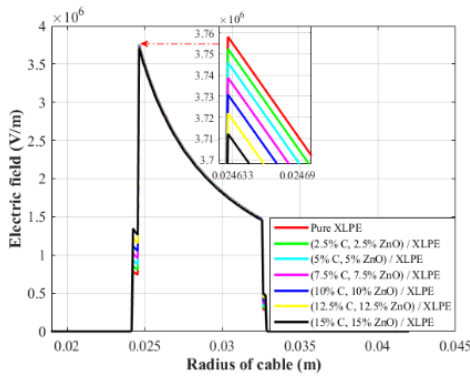


Fig. 13. Effect of natural graphite and zinc oxide in the insulating layer on the electric field behaviour in the cable

In the area corresponding to the insulating part of the high-voltage cable ($x: 0.0245 - 0.0325 \text{ m}, y: 0 - 0.042 \text{ m}$), where the electric field distribution is maximum, it is observed that the electric field distribution decreases with increasing concentration of the individual and multiple additive materials, as the electric field intensity of pure cross-linked polyethylene, in this case, reaches 3758.066 kV/m , it decreases as a function of natural graphite, zinc oxide, and multiple, it reaches 3700.590 kV/m

approximately 1.53% , 3722.244 kV/m around 0.953% and 3712.276 kV/m about 1.218% , respectively, at 30% of the concentration of additive materials.

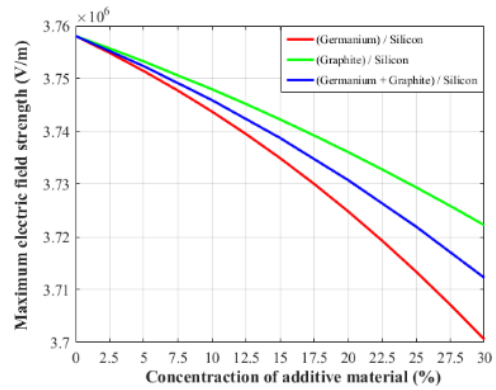


Fig. 14. The maximum electric field strength in the insulating layer as a function of additive materials concentration

4.2.3. The effect of additive materials in the outer semiconducting layer

In order to study the impact of additive materials in the external semiconducting layer on the electric field behaviour in the cable. Figures (15, 16, 17) illustrate the electric field behaviour inside high voltage underground cables by adding additive materials with several concentrations, which the variant is the external semi-conductive layer of pure silicon (Si) and composites with germanium (Ge), natural graphite (C), and multiple, respectively.

Figures (18, 19) show the maximum electric field strength in the external semiconducting layer and the insulating layer, respectively, as a function of additive material concentration.

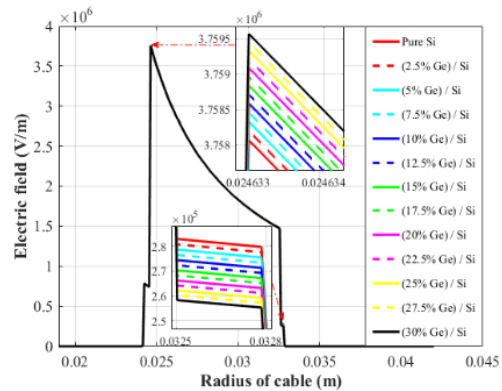


Fig. 15. Effect of germanium in the external semiconducting layer on the electric field behaviour in the cable

In the area corresponding to the external semiconducting ($x: 0.0325 - 0.0328 \text{ m}, y: 0 - 0.042 \text{ m}$), it can be seen that the electric field distribution decreases with increasing concentration of the individual and multiple additive materials; as the electric field strength in the case of pure silicon reaches 279.755 kV/m in this area, it decreases as a function of germanium, natural graphite, and

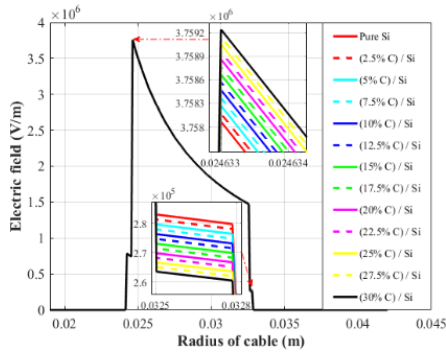


Fig. 16. Effect of natural graphite in the external semiconducting layer on the electric field behaviour in the cable

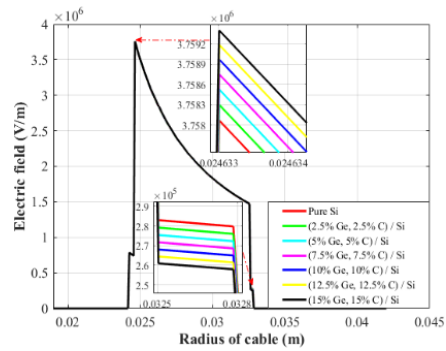


Fig. 17. Effect of germanium and natural graphite in the external semiconducting layer on the electric field behaviour in the cable

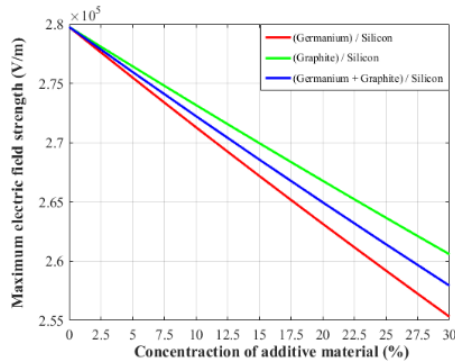


Fig. 18. The maximum electric field strength in the external semiconducting layer as a function of additive materials concentration

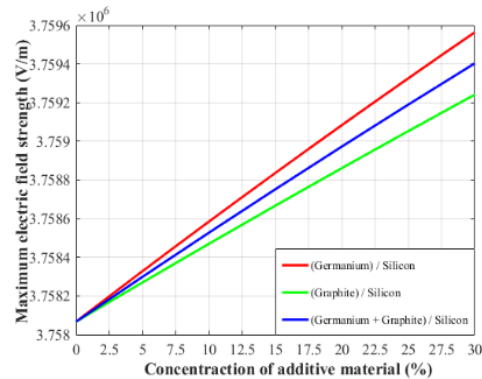


Fig. 19. The maximum electric field strength in the insulating layer as a function of additive materials concentration

multiple, it reaches 255.329 kV/m approximately 8.73 %, 260.591 kV/m around 6.85 %, and 257.944 kV/m about 7.79 %, respectively, at 30 % of the concentration of additive materials. However, in the area corresponding to the insulating part of the high-voltage cable (x: 0.0245 – 0.0325 m, y: 0 – 0.042 m), where the electric field distribution is maximum, it can be seen that the electric field distribution increases with increasing concentration of the individual and multiple additive materials as the electric field strength in the case of pure silicon reaches 3758.066 kV/m in this area, it increases as a function of germanium, natural graphite, and multiple, it reaches 3759.563 kV/m approximately 0.039 %, 3759.241 kV/m around 0.031 %, and 3759.403 kV/m close to 0.035 %, respectively, at 30 % of the concentration of additive materials.

4.2.4. The effect of additive materials in the common screen and the outer sheath layers

In order to study the impact of additive materials in the common screen layer and the outer sheath layer on the electric field behaviour in the cable.

Figures (20, 21) illustrate the electric field behaviour inside high-voltage underground cables by adding additive materials with different concentrations, which the variant is the common screen layer of pure ethylene propylene rubber (EPR), and a composite of natural graphite (C) and the outer sheath layer of pure polyvinyl chloride (PVC), and a composite of natural graphite (C), respectively.

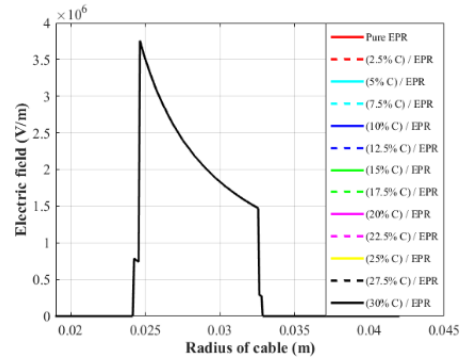


Fig. 20. Effect of natural graphite in the common screen layer on the electric field behaviour in the cable

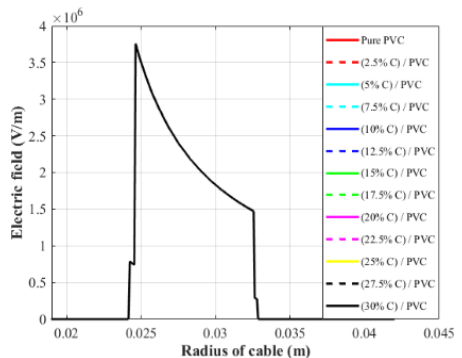


Fig. 21. Effect of natural graphite in the outer sheath layer on the electric field behaviour in the cable

According to the (Figures 20, 21), it can be seen that the increase in the concentration of the individual additive materials doesn't affect the electric field distribution in the cable since the electric potentials are grounded in the common screen layer. Therefore, the electric field distribution in these layers (common screen and outer sheath) is null. The maximum electric field strength around the cable is 3755.623 kV/m. In this case, we have studied the effect of other individuals (ZnO) and multiple (C + ZnO) additive materials. Still, as long as the additive materials don't influence the electric field distribution in the cable and for this reason, only the effect of natural graphite was shown.

5. CONCLUSION

The electrical characterisation of an underground high-voltage power cable can be simulated and analysed using numerical modelling with great accuracy and reduced computational time.

The study shows how this investigation can be performed with the finite element method implemented and solved efficiently by COMSOL Multiphysics software.

The addition of single or multiple particles to the pure materials corresponding to the different layers of the underground high-voltage power cable changes the dielectric constant of the material and affects the electric field distribution in the underground high voltage power cable.

Using individual and multi-composite materials instead of pure materials decreases the electric field distribution depending on the concentration of the individual or multiple additive materials. As the additive particle has high dielectric permittivity, the decrease of the electric field distribution in the corresponding layers in the underground high voltage cable is considerable.

The reduction of the electric field distribution as a function of the concentration of individual or multiple additive materials in the insulating layer is the most important compared to the other underground high-voltage electric cable layers.

Adding single or multiple particles to the pure materials in the internal and external semiconducting layers increase the electric field distribution in the insulating layer significantly.

Adding single or multiple particles to the pure materials of the different dielectric layers that come after the power cable's outer semiconducting layer doesn't affect the electric field distribution because the electric potentials at the common screen layer are grounded.

Source of funding: *This research received no external funding.*

Author contributions: *research concept and design, F.H.; Collection and/or assembly of data, N.G., L.M.; Data analysis and interpretation, F.H., H.N.; Writing the*

article, F.H.; Critical revision of the article, H.N., L.M., S.B.; Final approval of the article, H.N.

Declaration of competing interest: *The authors declare that they have no known competing financial interests or personal relationships that could have appeared to influence the work reported in this paper.*

REFERENCES

- Ocloń P, Bittelli M, Cisek P, Kroener E, Pilarczyk M, Taler D, et al. The performance analysis of a new thermal backfill material for underground power cable system. *Applied Thermal Engineering* 2016; 108: 233–50. <https://doi.org/10.1016/j.applthermaleng.2016.07.102>.
- Santos M, Calafat MA. Dynamic simulation of induced voltages in high voltage cable sheaths: Steady state approach. *International Journal of Electrical Power & Energy Systems* 2019; 105: 1–16. <https://doi.org/10.1016/j.ijepes.2018.08.003>.
- Han S, Sung M, Jang J, Jeon SY, Yu WR. The effects of adhesion on the tensile strength of steel-polymer sandwich composites. *Advanced Composite Materials* 2021; 30(5): 443–61. <https://doi.org/10.1080/09243046.2020.1835793>.
- Mansour DEA, Abdel-Gawad NMK, El Dein AZ, Ahmed HM, Darwish MMF, Lehtonen M. Recent advances in polymer nanocomposites based on polyethylene and polyvinylchloride for power cables. *Materials* 2020;14(1): 66. <https://doi.org/10.3390/ma14010066>.
- Abdel-Gawad NMK, El Dein AZ, Mansour DEA, Ahmed HM, Darwish MMF, Lehtonen M. Multiple enhancement of PVC cable insulation using functionalized SiO₂ nanoparticles based nanocomposites. *Electric Power Systems Research* 2018; 163: 612–25. <https://doi.org/10.1016/j.epsr.2017.11.011>.
- Abdul Razak NI, Yusoff NISM, Ahmad MH, Zulkifli M, Wahit MU. Dielectric, mechanical, and thermal properties of crosslinked polyethylene nanocomposite with hybrid nanofillers. *Polymers* 2023; 15(7): 1702. <https://doi.org/10.3390/polym15071702>.
- Guo M, Frechette M, David E, Demarquette NR, Daigle JC. Polyethylene/polyhedral oligomeric silsesquioxanes composites: Electrical insulation for high voltage power cables. *IEEE Transactions on Dielectrics and Electrical Insulation* 2017; 24(2): 798–807. <https://doi.org/10.1109/TDEI.2017.006144>.
- Su J, Du B, Li J, Li Z. Electrical tree degradation in high-voltage cable insulation: progress and challenges. *High Voltage* 2020; 5(4): 353–64. <https://doi.org/10.1049/hve.2020.0009>.
- Nawar A, Said A, Eldesoky E, Abdallah M. High Voltage cross-linked polyethylene insulator characteristics improvement using functionalized ZnO nanoparticles. *Egyptian Journal of Chemistry* 2020; 63(12): 4929-4939. <https://doi.org/10.21608/ejchem.2020.31244.2664>.
- Kim SJ, Ji KH, Paik SH. Numerical simulation of mechanical behavior of composite structures by supercomputing technology. *Advanced Composite Materials* 2008; 17(4): 373–407. <https://doi.org/10.1163/156855108X385339>.
- Pleşa I, Notingher PV, Stancu C, Wiesbrock F, Schlögl S. Polyethylene Nanocomposites for Power Cable

- Insulations. *Polymers* 2018; 11(1): 24. <https://doi.org/10.3390/polym11010024>.
12. Hsissou R, Seghiri R, Benzekri Z, Hilali M, Rafik M, Elharfi A. Polymer composite materials: A comprehensive review. *Composite Structures* 2021; 262: 113640. <https://doi.org/10.1016/j.compstruct.2021.113640>.
 13. Said A, Abd-Allah MA, Nawar AG, Elsayed AE, Kamel S. Enhancing the electrical and physical nature of high-voltage XLPE cable dielectric using different nanoparticles. *Journal of Materials Science: Materials in Electronics* 2022; 33(10): 7435–43. <https://doi.org/10.1007/s10854-022-07868-9>.
 14. Said AR, Nawar AG, Elsayed AE, Abd-Allah MA, Kamel S. Enhancing electrical, thermal, and mechanical properties of HV cross-linked polyethylene insulation using silica nanofillers. *Journal of Materials Engineering and Performance* 2021; 30(3): 1796–807. <https://doi.org/10.1007/s11665-021-05488-8>.
 15. Essawi S, Nasrat L, Ismail H, Asaad J. Effect of nanoparticles on dielectric, mechanical and thermal characteristics of XLPE/TiO₂ nanocomposites. *International Journal of Advanced Technology and Engineering Exploration* 2021; 8(83): 1243-1254. <https://doi.org/10.19101/IJATEE.2021.87434>.
 16. Thomas J, Joseph B, Jose JP, Maria HJ, Main P, Rahman AA, Francis B, Ahmad Z, Thomas S. Recent advances in cross-linked polyethylene-based nanocomposites for high voltage engineering applications: a critical review. *Industrial & Engineering Chemistry Research* 2019; 58(46): 20863-20879. <https://doi.org/10.1021/acs.iecr.9b02172>.
 17. Wang Y, Wang C, Xiao K. Investigation of the electrical properties of XLPE/SiC nanocomposites. *Polymer Testing* 2016; 50: 145-151. <https://doi.org/10.1016/j.polymertesting.2016.01.007>.
 18. Shanghai Shenghua Cable (Group) Co., Ltd; 1997. High voltage three phase XLPE insulated steel wire armoured electrical cable CU/ XLPE/SWA/PVC power cable 33 kV; Available from <https://www.shanpowercable.com/sale-10130486-high-voltage-three-phase-xlpe-insulated-steel-wire-armoured-electrical-cable-cu-xlpe-swa-pvc-power-c.html>
 19. Abarna D, Vigneshwaran B, Willjuice Iruthayarajan M, Maheswari RV. Influence the effect of cavity size and position in high voltage cable by using finite element method. *International Journal of Scientific & Technology Research* 2020; 9: 5.
 20. Eranna Golla. *Crystal growth and evaluation of silicon for VLSI and ULSI*. Boca Raton FL: CRC Press; 2015.
 21. Vahedy V. Polymer insulated high voltage cables. *IEEE Electrical Insulation Magazine* 2006; 22(3): 13-18. <https://doi.org/10.1109/MEI.2006.1639025>.
 22. Moore George F. *Electric cables handbook*. 3rd ed Blackwell Science; 1997.
 23. Kruželák J, Kvasničáková A, Hložeková K, Hudec I. Progress in polymers and polymer composites used as efficient materials for EMI shielding. *Nanoscale Advances* 2021; 3(1): 123–72. <https://doi.org/10.1039/D0NA00760A>.
 24. Chung KT, Sabo A, Pica AP. Electrical permittivity and conductivity of carbon black-polyvinyl chloride composites. *Journal of Applied Physics* 1982; 53(10): 6867–79. <https://doi.org/10.1063/1.330027>.
 25. Alemour B, Yaacob MH, Lim HN, Hassan MR. Review of electrical properties of graphene conductive composites. *International Journal of Nanoelectronics & Materials* 2018; 11(4) :371-398.
 26. Khouildi E, Rabah A, Nejib C. Numerical modeling of the electric field and the potential distributions in heterogeneous cavities inside XLPE power cable insulation. *Journal of Electrical and Electronics Engineering* 2016; 9(2): 37.
 27. Calame JP, Birman A, Carmel Y, Gershon D, Levush B, Sorokin AA, et al. A dielectric mixing law for porous ceramics based on fractal boundaries. *Journal of Applied Physics* 1996; 80(7): 3992–4000. <https://doi.org/10.1063/1.363357>.
 28. Tuncer E, Serdyuk YV, Gubanski SM. Dielectric mixtures: electrical properties and modeling. *IEEE Transactions on Dielectrics and Electrical Insulation* 2002; 9(5): 809–28. <https://doi.org/10.1109/TDEI.2002.1038664>.
 29. Zakri T, Laurent JP, Vauclin M. Theoretical evidence for 'Lichtenecker's mixture formulae' based on the effective medium theory. *Journal of Physics D: Applied Physics* 1998; 31(13): 1589–94. <https://doi.org/10.1088/0022-3727/31/13/013>.
 30. Roy I, Lewis R, Marya MP, Ganguly P, Inventor; Schlumberger Technology Corporation, Texas, assignee. Evaluation of Low Resistivity Low Contrast Productive Formations. United States patent US 13/796,727. 2014 Apr.
 31. Chen SJ, Liu YC, Jiang H, Lu YM, Zhang JY, Shen DZ, et al. Raman and photoluminescence studies on nanocrystalline ZnO grown on GaInPAs substrates. *Journal of Crystal Growth* 2005; 285(1–2): 24–30. <https://doi.org/10.1016/j.jcrysgro.2005.07.036>.



Faouzi HASSAINE

Received an M.S. degree in Electrical Engineering from the University of Ferhat Abbas Setif 1, Algeria, in 2019. Currently, he is working toward the Ph.D. degree in Electrical Engineering at the University of Ferhat Abbas Setif 1, Algeria. His interests include Power Systems and High Voltage Engineering. In addition, his

research focuses on the High Voltage Underground Cables.

E-mail: faouzi.hassaine@univ-setif.dz & faouzihassaine123@gmail.com



Lakhdar MADANI

Obtained an engineering degree in electronics in 2001 at the University of Setif in Algeria. In 2016, the University of Setif will award the doctorate. In electrical engineering. He is currently a principal research professor at the DAC-HR Laboratory (Dosage analysis and characterization in high resolution) at the University of

Setif. His research interests include high voltage electrical and electro-energy system and renewable energy.

E-mail: madani_lakhdar10@yahoo.fr



Nacereddine GUETTAF was Born in Setif, Algeria. He received M.S degrees in electrical engineering from the University of Ferhat Abbas Setif1, Setif, Algeria, in 2018. He is currently working toward the Ph.D. degree in electrical engineering at the University of Ferhat Abbas Setif1, Setif, Algeria. His current research interests include Power

Systems, High Voltage Engineering, application of Corona Discharge, and Electrostatics Phenomena.

E-mail: nacer562eddine@gmail.com



Samira BOUMOUS.

Presently she is Associate Professor in Department of Electrical Engineering, University of Mohamed-Cherif Messaadia of Souk Ahras, Algeria. Member in Electrotechnics and Renewable energy Laboratory (LEER). His fields of interest are Power system, high voltage, Microgrid, FACTS.

E-mail: samira.boumous@univ-soukahras.dz



Hamou NOURI

Received the Ph.D. degree in electrical engineering from Bejaia University, Béjaïa, Algeria, in 2010, and then, the “Habilitation à Diriger de Recherches” Diploma degree in electrical engineering in 2012. He is currently a Professor with the Department of Electrical Engineering, Setif University, Setif, Algeria. His research

interests include the application of corona discharge, nonthermal plasma technology, and air pollution control, as well as the mathematical modeling of electrostatics systems.

E-mail: nouri_hamou@yahoo.fr